Available online at www.sciencedirect.com
SCIENCE DIRECT®
Journal of Nuclear Materials 342 (2005) 141–147
journal of nuclear materials
www.elsevier.com/locate/jnucmat

Bombardment of graphite with hydrogen isotopes: A model for the energy dependence of the chemical sputtering yield

C. Hopf, W. Jacob *

EURATOM Association, Max-Planck-Institut für Plasmaphysik, Boltzmannstr. 2, 85748 Garching, Germany

Received 5 January 2005; accepted 5 April 2005

Abstract

Carbon materials inside magnetic-confinement nuclear fusion devices are eroded by hydrogen ions and atoms. Even at room temperature, where thermal chemical erosion is negligible, erosion does not cease below the energy threshold for physical sputtering. The effect, which requires both chemical reactivity and hyperthermal energy of the eroding species, is known as 'chemical sputtering'. Based on a concept of the underlying microscopic mechanism we have previously developed a model for the energy-dependent yield of chemical sputtering due to simultaneous impact of thermal atomic hydrogen and energetic noble gas ions. In the present article the model is adapted to the case of pure hydrogen ion bombardment of graphite yielding good quantitative and qualitative agreement with published data. Especially, the large isotope effect below 100 eV comparing deuterium and hydrogen ion bombardment is well reproduced and its origin is discussed. Additionally, the chemical sputtering yield is calculated for tritium ions.

1. Introduction

Carbon is among the favorite materials for the first wall of magnetic-confinement nuclear fusion experiments due to its favorable thermo-mechanical properties as well as its low nuclear charge. However, its use in next-step devices and future commercial reactors is threatened by the high erosion rates observed in present day machines and dedicated laboratory erosion experiments [1].

The erosion of carbon due to hydrogen species can be classified into three regimes: (i) Thermal chemical erosion at elevated temperatures above approximately 400 K with a maximum at ≃600 to 900 K due to thermal atomic [2] or energetic (e.g. [3,4]) hydrogen while thermal molecular hydrogen does not react with the surface [2], (ii) physical sputtering due to energetic species impact above a specific threshold energy [5], and (iii) chemical sputtering due to energetic hydrogen species or a combination of atomic hydrogen and any other energetic species (e.g. [6,7,4]). Chemical sputtering can be observed even below the threshold energy for physical sputtering and at room temperature where neither of the first two erosion mechanisms contributes.

We have recently investigated chemical sputtering of amorphous hydrocarbon (a-C:H) films at 340 K [8,9]. The films were bombarded with Ar^+ or H_2^+ ions while simultaneously exposing them to an atomic hydrogen beam the flux density of which exceeded that of the ions by a factor of 100–500. This approach offered the advantage that the influence of the energetic minority species

* Corresponding author. Tel.: +49 89 3299 2617/2618; fax: +49 89 3299 1149.
E-mail address: wolfgang.jacob@ipp.mpg.de (W. Jacob).

0022-3115/$ - see front matter © 2005 Elsevier B.V. All rights reserved.
doi:10.1016/j.jnucmat.2005.04.003

could be studied while keeping the supply of the chemically reactive majority species constant. We concluded from the energy dependence of the erosion yield, i.e., the number of carbon atoms eroded per incident ion, that the underlying microscopic mechanism is not the sputtering of weakly bound hydrocarbons at the surface, as proposed by Roth et al. [10,11] and widely accepted (e.g. [12]). Instead, our results could be consistently explained by the following mechanism of chemical sputtering: Energetic ions break C–C bonds within their penetration range in the carbon material and the resulting dangling bonds are passivated by the hydrogen atoms. Consecutive bond breaking and passivation lead to the formation of volatile hydrocarbons at and below the surface which diffuse to the surface and desorb.

Based on this mechanism we have described the energy dependence of the chemical sputtering yield in the case of simultaneous ion and atomic hydrogen bombardment by [9]

$$Y_{\mathrm{cs}}(E) = a \int y_{\mathrm{bb}}(x,E)\mathrm{e}^{-x/\lambda}\,\mathrm{d}x. \qquad (1)$$

Herein, $y_{\mathrm{bb}}(x,E)$ is the number of bond-breaking events per incident ion and unit depth interval around depth x. It is estimated by TRIM.SP [13] calculations for a given ion energy E counting the number of 'carbon-displacement' events. In our view, however, $y_{\mathrm{bb}}(x,E)$ is not associated with displacement but with bond breaking. Accordingly, we replace the TRIM.SP displacement energy for C by a bond-breaking energy E_{bb} which is the minimum amount of energy that has to be transferred to a target C atom to break a C–C bond. It was chosen within the range of typical C–C bond energies in hydrocarbon molecules as 5 eV. The exponential function $\exp(-x/\lambda)$ serves as the passivation probability of dangling bonds due to atomic hydrogen at depth x. As thermal H is known to penetrate roughly 2 nm into a-C:H [14,15] $\lambda = 0.4$ nm was chosen. The total yield is then given by the overlap of y_{bb} and $\exp(-x/\lambda)$, i.e., the integral over the product, Eq. (1). The quantity y_{bb} is an absolute number in units of events per nanometer. Concerning the passivation probability we only demand that it must be smaller than one. Additional dependences, e.g., the dependence of Y on the ratio of H and ion fluxes, are contained in the additional scaling parameter a which is constant if only E is varied. With $a = 0.4$ Eq. (1) describes the energy-dependent yield of our experiments with both Ar^+ and H_2^+ ions and simultaneous thermal H exposure very satisfactorily [9].

2. Computation

As noted above, experiments using low-energy ions, preferably chemically non-reactive ions such as argon, together with an excess flux of thermal atomic hydrogen offer significant advantages when trying to unravel the microscopic mechanism of chemical sputtering. Indeed, hydrogen ion bombardment in a plasma environment will always be accompanied by a certain flux of thermal hydrogen atoms. On the other hand, chemical sputtering due to hydrogen ions (H^+, H_2^+, H_3^+, D^+, ...) as the only interacting species is also of high practical relevance to nuclear fusion research as it represents the other extreme with no or negligible contribution of thermal H. For the latter case a plethora of data exists from dedicated erosion experiments using both mass spectrometers [16–19,7] to quantitatively determine the fluxes of erosion products and microbalances to measure the target's weight loss during the experiment [6,10,11,4]. The latter experiments provide the most reliable information on the total chemical sputtering yield. The total change of weight of a graphite target is measured during the experiment and compared to the ion fluence. When using molecular ions in these experiments it is generally assumed that an H_x^+ ion with an incident energy E_0 is equivalent to x H^+ ions at E_0/x. As our model does not account for thermal chemical erosion we only consider measurements at room temperature in this article.

Fig. 1 shows the energy-dependent erosion yield (eroded C per incident H or D) from weight-loss measurements for both H^+ (solid symbols) and D^+ (open symbols) bombardment of various types of graphite at room temperature. The data were taken from a compilation by Balden and Roth (Fig. 3 in [4]). At incident ion energies above roughly 300 eV, the yields can be entirely explained by physical sputtering. The dash-dotted lines in Fig. 1 show the results of TRIM.SP calculations of the physical sputtering yields. As target material in the calculations carbon with a density of 2.22×10^3 kg m^{-3} was assumed which contained 1% of hydrogen for technical reasons of the calculation. The surface binding energy of C was set to 7.4 eV [13]. The calculated yields are somewhat smaller than the experimental ones. Küstner et al. [20] have shown that the difference is due to the roughness of the real graphite surface. Instead of explicitly taking surface roughness into account, in some works simply a reduced surface binding energy of 4.4 eV is used to reproduce experimental yields [21]. However, a disadvantage of this procedure is that reducing the surface binding energy also shifts the threshold energy of physical sputtering to lower values. Therefore we have chosen the value of 7.4 eV although neglecting roughness. Apart from the resulting slight underestimation the calculated physical sputtering yields show good agreement with the data above approximately 300 eV.

Below about 300 eV the calculation predicts a steep decrease of the physical sputtering yield with decreasing energy and no sputtering at all is expected below ≈50 eV for H^+ and ≈30 eV for D^+. In contrast, the measured yields show no such decrease down to 15 eV. In this

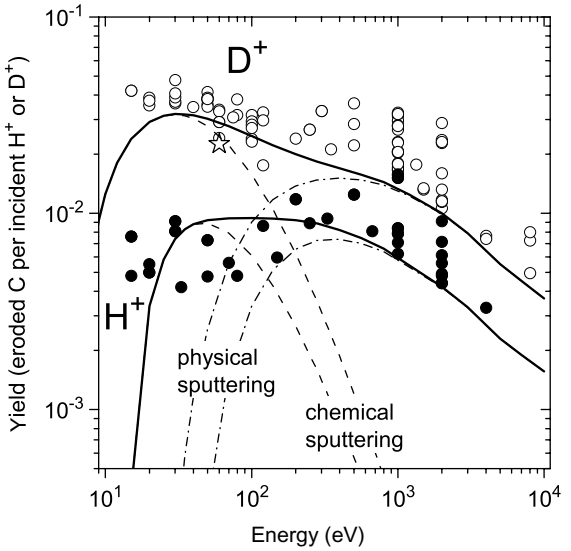

Fig. 1. Impact energy dependence of the total erosion yield of graphite bombarded with hydrogen or deuterium ions at room temperature. The open and solid symbols are measured yields taken from Ref. [4] for D^+ and H^+ bombardment, respectively. They were obtained via weight loss measurements during D_3^+ or H_3^+ bombardment at three times the energy given on the abscissa, and the yield was calculated by $Y = \Delta N/(3 \times F)$, where ΔN is the number of C atoms eroded and F the fluence of H_3^+ or D_3^+ ions. The open star was measured with D^+ instead of D_3^+. The lines show the physical sputtering yield calculated with TRIM.SP (dash-dotted), the chemical sputtering yield according to Eq. (3) (dashed), and the sum of chemical and physical sputtering (solid).

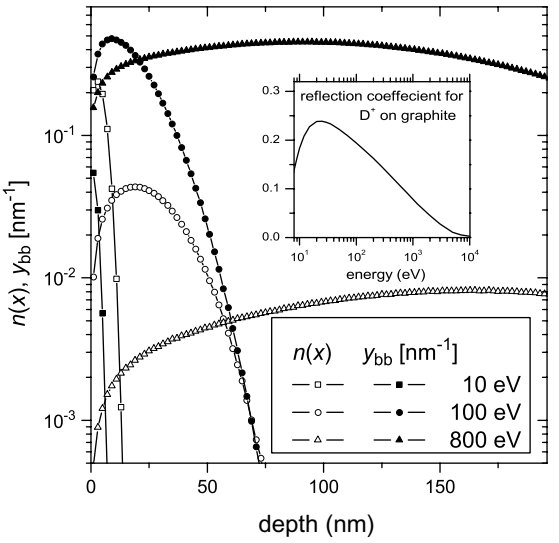

Fig. 2. Implantation depth profile $n(x)$ (open symbols) and bond-breaking yield density $y_{bb}(x)$ (solid symbols) of D^+ ions at three different impact energies calculated with TRIM.SP. The inset shows the energy dependence of the projectile reflection coefficient for D^+.

low-T, low-E regime chemical sputtering is the dominant erosion mechanism.

In order to apply the model expressed in Eq. (1) some modifications are necessary because now the ions provide both the damage and the chemical reactivity. As before, the total yield will be proportional to the overlap of damage and passivation probability. The latter depends on the depth-dependent availability of hydrogen which in the ions plus thermal H case was constant due to the energy-independent H supply. Now the availability of hydrogen is given by the energy-dependent implantation depth profile $n(x, E)$ of the H^+ or D^+ ions. Hence, the most straight forward modification of Eq. (1) is to replace the exponential function by the ion range distribution $n(x, E)$ as calculated by TRIM.SP. The chemical sputtering yield reads

$$Y_{cs}(E) = a \int y_{bb}(x, E) n(x, E)\, dx. \quad (2)$$

Comparing $n(x, E)$ and $y_{bb}(x, E)$ at different ion energies (see Fig. 2) it becomes immediately obvious that this equation is not suitable for reproducing the data: The shape of both functions develops very similarly. Particle conservation demands that $\int n(x, E)\, dx$ is constant; taking projectile reflection (inset in Fig. 2) into account, $\int n(x, E)\, dx$ even increases by about 30% from 20 to 10 000 eV. At the same time, the total number of bond-breaking events $\int y_{bb}(x, E)\, dx$ increases significantly with energy. Consequently, the integral in Eq. (1) increases monotonously with energy in contrast to the experiment: the chemical sputtering yield Y_{cs} is the difference between the measured erosion yields and the calculated physical sputtering yields which decreases where physical sputtering becomes effective.

Obviously, we have to introduce a term into Eq. (2) which restricts the process to a near-surface region. We have pointed out in Ref. [9] that the interpretation of the term $\exp(x/\lambda)$ as passivation probability, with λ being a typical range of thermal atomic hydrogen in a-C:H, is not unique. In the light of this discussion we tend to interpret $\exp(x/\lambda)$ as the depth-dependent probability for the out-diffusion of erosion products formed at depth x, in accordance with what we have suggested alternatively in Ref. [9]. This allows us to re-introduce the term into Eq. (2). Finally, we obtain

$$\begin{aligned} Y_{tot}(E) &= Y_{cs}(E) + Y_{phys}(E) \\ &= a \int y_{bb}(x, E) n(x, E) e^{-x/\lambda}\, dx + Y_{phys} \end{aligned} \quad (3)$$

for the total erosion yield including physical sputtering. Y_{cs} and Y_{tot} were calculated by TRIM.SP using again 5 eV as carbon-displacement energy and $\lambda = 0.4$ nm. The surface-binding energy of the projectile on graphite

was chosen as the desorption energy of hydrogen from a fully H-covered graphite (0001) surface [22], which is 3.3 eV. It becomes important at low energies as the projectile's initial energy is increased by this value when approaching the surface. The target composition and density were chosen like for the calculation of the physical sputtering yield, see above. The depth distributions $y_{bb}(x,E)$ and $n(x,E)$ were calculated with 2 nm depth resolution and the integral was approximated as discrete sum with x being the mean depth in each interval.

Y_{cs} and Y_{tot} with $a = 1$ are shown in Fig. 1 as dashed and solid lines, respectively, again for both isotopes. Considering the simplicity of the model expressed in Eq. (3) the agreement with the data is good.

3. Discussion

3.1. Magnitude

The yield density $y_{bb}(x,E)$ is the absolute number of broken C–C bonds per unit depth-interval in units of nm^{-1}. The dimensionless quantity $n(x,E)$ is the absolute number of hydrogen ions implanted into a 1 nm depth interval around depth x. Finally, $\exp(-x/\lambda)$ plays the role of a depth-dependent probability which has to be $\leqslant 1$ everywhere. Thus, we expect a priori that the integral on the right-hand side in Eq. (3) gives the correct order of magnitude for the chemical sputtering yield. However, the average number of implanted H needed in the vicinity of a bond-breaking event as well as the average number of bond-breaking events necessary to erode one C are not known, although it is reasonable to expect both quantities in the range from 1 to 10. All we know about the probability for out-diffusion of erosion products is that it will be unity at the very surface and approach zero for $x \to \infty$. Considering these uncertainties, we allowed for a scaling factor a in Eq. (3). However, in contrast to applying Eq. (3) to our Ar^+/H and H_2^+/H data [9] where $a = 0.4$ gave best agreement, $a = 1$ leads to the very good agreement in Fig. 1.

3.2. Isotope effect

Looking at the data in Fig. 1 one distinctive feature is the increase of the isotope effect (i.e., the ratio of the D^+ and H^+ yields) with decreasing energy; while the D^+ yield even increases from 100 down to 15 eV, the H^+ yield is constant or even decreases a little. This basic feature is essentially reproduced by our model calculation. The absolute difference between H^+ and D^+ yields seems somewhat underestimated by the model although the model curves both lie within the scatter of the data. In our model the isotope effect and the fact that it is more pronounced at lower energies result from the following dependences:

(i) The collisional energy transfer is different for different projectile masses. The maximum transferable energy in a head-on collision is given by the kinematic factor $\gamma(M_1,M_2) = 4M_1M_2/(M_1+M_2)^2$ where M_1 and M_2 are the projectile and target masses. For collisions with carbon the ratio of the kinematic factors for deuterium and protium projectiles is $\gamma(M_D,M_C)/\gamma(M_H,M_C) \approx 1.7$. This number must not be confused with the ratio of the corresponding physical sputtering yields, but it gives an idea of the magnitude of the isotope effect. Indeed, both in the experiment and in the TRIM.SP calculations a ratio $Y_{phys}(D)/Y_{phys}(H) \approx 2$ is found.

(ii) There is less implantation of H in the near surface region compared to D due to the difference in the penetration range distribution. For D the factor $n(x,E)$ is therefore larger close to the surface, where $\exp(-x/\lambda)$ allows out-diffusion of the erosion products.

(iii) Due to the need to transfer a certain minimum amount of energy to a carbon atom to break a bond, $E_{bb} = 5$ eV in our case, there is an energy threshold $E_{th} = E_{bb}/\gamma(M_1,M_C)$ below which the chemical sputtering yield becomes zero. This threshold is lower for D^+ than for H^+. Consequently, the isotope effect increases when approaching the threshold from the high-energy side and becomes infinity below the threshold for protons.

Point (iii) makes clear that the term describing damage production must be associated with a process that has such an energy threshold in order to reproduce the large isotope effect at low energies. The effect is visualized in Fig. 3 where two different choices for the damage term are compared. In the first case the integral $\int f(x,E)n(x,E)\exp(-x/\lambda)\,dx$ was calculated with $f(x,E)$ being the carbon bond-breaking yield density as in Eq. (3) (solid line). In the second case the total nuclear energy deposition function $f_d(x,E)$, i.e., the energy transferred in both projectile–target and target–target elastic collisions, was used instead (dashed line). In the latter case no energy threshold is involved. A different proportionality constant a_{f_d} has to be used which was chosen such that the two models coincide at 100 eV. Whereas the difference between the two models is negligible above 100 eV the model using f_d continues to increase down to 10 eV and shows a far less pronounced isotope effect at low energies.

One of the a priori choices for the model was that of a carbon–carbon bond breaking energy of 5 eV. Being a typical value of a C–C bond energy in hydrocarbons it seems a very reasonable choice for a-C:H films [9] and the near surface of graphite modified by hydrogen bombardment [23,24]. However, molecular dynamics

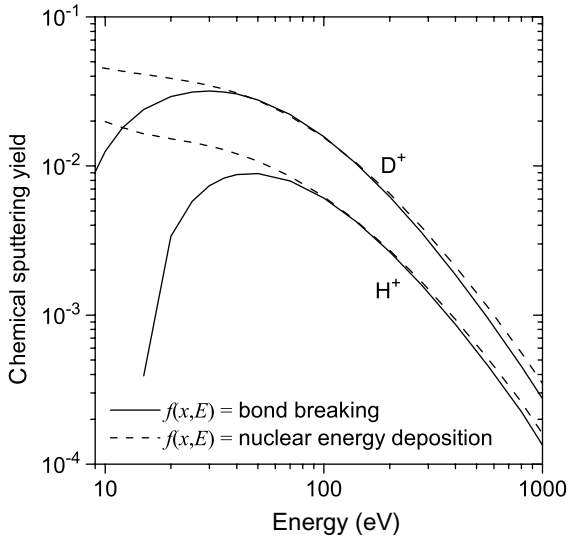

Fig. 3. Comparison between chemical sputtering models $Y_{cs} = \int f(x,E) n(x,E) e^{-x/\lambda} dx$ using different damage functions f; solid line: $f = y_{bb}$; dashed line: f = nuclear (elastic) energy deposition function.

calculations have shown that protons can eventually cause C–C bond breaking down to 1 eV [25]. The influence of the bond breaking energy E_{bb} is visualized in Fig. 4. As the absolute values of Y_{cs} decrease with increasing E_{bb} different constants $a = 0.134$ and 1.6055 were used for $E_{bb} = 1$ and 7 eV, respectively, so that the D^+ yields are all equal at 100 eV. Apart from this general scaling the threshold energies increase with E_{bb} and, hence, the isotope effect at a given energy becomes more pronounced. Comparison with the data in Fig. 1 restricts the choice of E_{bb}: the large isotope effect rules out low values whereas the obviously low threshold <10 eV for both D^+ and H^+ demands a not too large E_{bb}. Choosing 5 eV appears to be a good compromise.

In a real system there will be no unique bond-breaking energy, especially not for a material disordered due to particle bombardment. Instead, a distribution of bond-breaking energies will exist depending on local environment and details of the collision. Assuming such a distribution agreement between data and model can be improved. Especially, when allowing only a small fraction of the C–C bonds to be broken at low transferred energies (e.g., 1% of the bonds at 1 eV) while for the majority E_{bb} is unchanged the yield remains high down to 10 eV, and at the same time a large isotope effect is maintained. However, having no independent knowledge on this distribution, introducing it into our calculations would result in a rather arbitrary model.

3.3. Predictions for tritium

The fuel in future nuclear fusion experiments and reactors will consist of equal amounts of deuterium and tritium. Unfortunately, due to the difficulties in handling tritium, no reliable erosion yield data exist to date for the chemical sputtering of graphite with tritium ions. Fig. 5 shows Y_{phys}, Y_{cs} and the total yield according to Eq. (3) calculated for T^+. For comparison Y_{tot} is also given for H^+ and D^+. As expected considering the higher mass, the T^+ yields are higher than those of D^+ and the

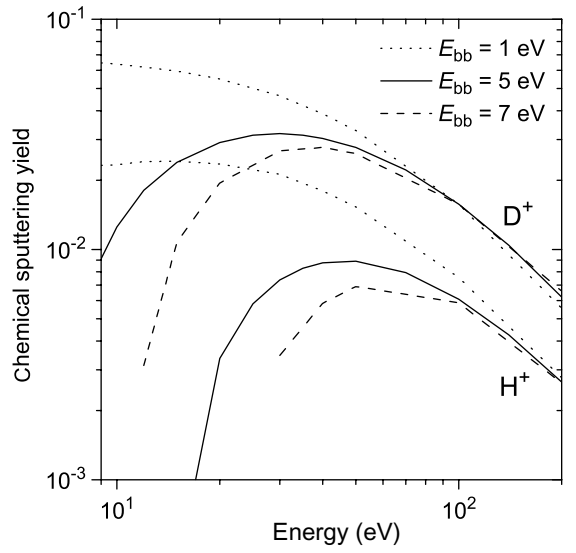

Fig. 4. Y_{cs} according to Eq. (3) calculated with different bond-breaking energies of 1, 5, and 7 eV.

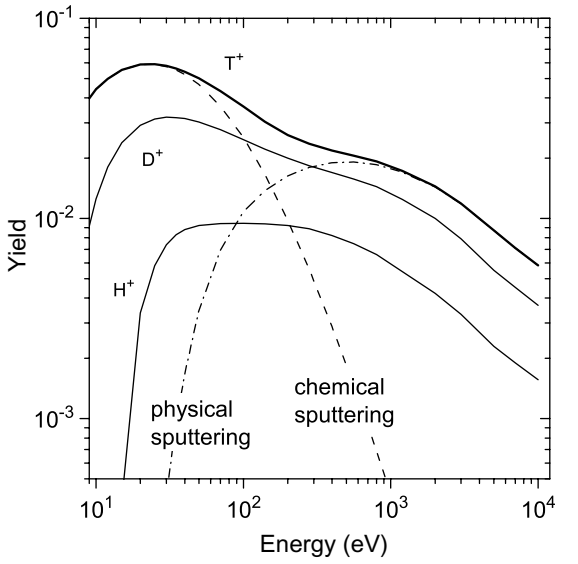

Fig. 5. Prediction for the chemical sputtering yield (dashed) and the physical sputtering yield (dash-dotted) for T^+ bombardment. The total yield is shown as thick solid line. For comparison the total yields for H^+ and D^+ are shown again.

thresholds are shifted to lower energies. However, the relative isotope effect between T and D is smaller than between D and H due to the smaller mass ratio. Still, the yield maximum of T^+ is by a factor of $\approx$1.8 higher than that of D^+ and $\approx$6 times higher than that of H^+.

3.4. Comparison with previous models

The general idea that low-energy room-temperature chemical sputtering of graphite due to hydrogen ions is caused by ion-induced damage together with chemical reactivity provided by slowed down ions is not entirely new. Möller and Scherzer briefly present a model in Ref. [26] to explain data by Roth [27]. In their description the chemical sputtering yield is $Y_{cs} = \text{constant} \times f_d(0,E) \times n(0,E)$, where $f_d(0,E)$ is the nuclear energy deposition function at the surface and $n(0,E)$ is the amount of hydrogen deposited at the very surface. Although their model shows a certain similarity with ours it cannot describe the increase of the isotope effect towards low energies because $f_d(0,E)$ has no energy threshold, as pointed out above.

Even earlier Yamada and Sone [28] presented a model which was based on previous work by Erents et al. [29] but additionally included the effect of ion damage. They assume that the chemical sputtering yield is proportional to the number of reactive sites in the surface layer as well as the concentration of hydrogen at the very surface. The production rate of reactive sites is assumed to be proportional to the 'recoil energy density' which is said to be proportional to the sputtering yield. They calculate the recoil energy density from computed physical sputtering yields. Consequently, their chemical sputtering yields become zero below the threshold of physical sputtering, in contradiction to the experiment. Yamada and Sone only present calculations and data down to 100 eV. The hydrogen concentration in their model is calculated by rate equations which consider the incident hydrogen ion flux, particle reflection, thermal desorption and ion-induced desorption. They do not account for the energy-dependent range distribution of the implanted hydrogen ions.

Möller's model and Yamada's model both assume that chemical sputtering is strictly limited to the very surface, i.e., the first monolayer. We also included the limitation to a near-surface region into our model through the probability of out-diffusion of the erosion products. However, our near-surface region is about 2 nm thick which corresponds to about ten monolayers. Indeed, subsurface molecule formation at the end of ion range was proven in experiments [30].

4. Summary

We presented a model for the impact energy dependence of the chemical sputtering yield in the case of H and D ion bombardment of carbon. Within this model the local chemical sputtering yield at a given depth is proportional to the number of hydrogen ions implanted into this depth and the number of C–C bond-breaking events. For the computations the corresponding bond-breaking energy was assumed to be 5 eV. Furthermore, the process is restricted to a near surface region, possibly by the depth-dependent probability for the erosion products to diffuse out of the film. The model gives the right magnitude of the yields; it also reproduces well the increase of the isotope effect towards lower energies. The isotope effect results from the different energy transfer in H–C and D–C collisions and the different range of H and D ions in the solid at a given energy. Additionally, the isotope effect becomes more pronounced in the proximity of the threshold energies for chemical sputtering.

References

[1] G. Federici, C.H. Skinner, J.N. Brooks, J.P. Coad, C. Grisolia, A.A. Haasz, A. Hassanein, V. Philipps, C.S. Pitcher, J. Roth, W.R. Wampler, D.G. Whyte, Nucl. Fusion 41 (2001) 1967.
[2] J. Küppers, Surf. Sci. Rep. 22 (1995) 249.
[3] E. Vietzke, V. Philipps, Fusion Technol. 15 (1989) 108.
[4] M. Balden, J. Roth, J. Nucl. Mater. 280 (2000) 39.
[5] R. Behrisch, Sputtering by Particle Bombardment I, 1st Ed., Springer, Berlin, 1981.
[6] J. Roth, J. Bohdansky, Nucl. Instrum. and Meth. B 23 (1987) 549.
[7] B.V. Mech, A.A. Haasz, J.W. Davis, J. Nucl. Mater. 255 (1998) 153.
[8] C. Hopf, A. von Keudell, W. Jacob, Nucl. Fusion 42 (2002) L27.
[9] C. Hopf, A. von Keudell, W. Jacob, J. Appl. Phys. 94 (2003) 2373.
[10] J. Roth, C. García-Rosales, Nucl. Fusion 36 (1996) 1647; see also corrigendum: J. Roth, C. García-Rosales, Nucl. Fusion 37 (1997) 897.
[11] J. Roth, J. Nucl. Mater. 266–269 (1999) 51.
[12] B.V. Mech, A.A. Haasz, J.W. Davis, J. Appl. Phys. 84 (1998) 1655.
[13] W. Eckstein, Computer simulation of ion–solid interactions, Springer Series in Materials Science, 1st Ed., Springer, Berlin, 1991.
[14] J. Pillath, J. Winter, F. Waelbroek, in: P. Koidl, P. Oelhafen (Eds.), Amorphous Hydrogenated Carbon Films, E-MRS Symposia Proceedings, vol. XVII, Les Editions de Physique, Paris, 1987, p. 449.
[15] A. von Keudell, W. Jacob, J. Appl. Phys. 79 (1996) 1092.
[16] J.W. Davis, A.A. Haasz, P.C. Stangeby, J. Nucl. Mater. 145–147 (1987) 417.
[17] J.W. Davis, A.A. Haasz, P.C. Stangeby, J. Nucl. Mater. 155–157 (1988) 234.
[18] A.A. Haasz, J.W. Davis, C. Wu, J. Nucl. Mater. 162–164 (1989) 915.
[19] A.A. Haasz, B.V. Mech, J.D. Davis, J. Nucl. Mater. 231 (1996) 170.

[20] M. Küstner, W. Eckstein, V. Dose, J. Roth, Nucl. Instrum. Meth. B 145 (1998) 320.
[21] W. Eckstein, A. Sagara, K. Kamada, J. Nucl. Mater. 150 (1987) 266.
[22] E. Ghio, L. Mattera, C. Salvo, F. Tommasini, U. Valbusa, J. Chem. Phys. 73 (1) (1980) 556.
[23] E. Vietzke, K. Flaskamp, V. Philipps, G. Esser, P. Wienhold, J. Winter, J. Nucl. Mater. 145–147 (1987) 443.
[24] E. Vietzke, V. Philipps, K. Flaskamp, J. Nucl. Mater. 162–164 (1989) 898.
[25] E. Salonen, K. Nordlund, J. Keinonen, C. Wu, Phys. Rev. B 63 (2001) 195415.
[26] W. Möller, B.M.U. Scherzer, Appl. Phys. Lett. 50 (1987) 1870.
[27] J. Roth, J. Nucl. Mater. 145–147 (1987) 87.
[28] R. Yamada, K. Sone, J. Nucl. Mater. 116 (1983) 200.
[29] S.K. Erents, C.M. Braganza, G.M. McCracken, J. Nucl. Mater. 63 (1976) 399.
[30] J. Roth, J. Bohdansky, Appl. Phys. Lett. 51 (1987) 964.